

# A Slotted Patch Antenna for Wireless Strain Sensing

Xiaohua Yi<sup>1</sup>, Chunhee Cho<sup>1</sup>, Benjamin Cook<sup>2</sup>, Yang Wang<sup>\*1</sup>, Manos M. Tentzeris<sup>2</sup>,  
Roberto T. Leon<sup>3</sup>

<sup>1</sup> School of Civil and Environmental Engineering, Georgia Institute of Technology,  
Atlanta, GA 30332, USA

<sup>2</sup> School of Electrical and Computer Engineering, Georgia Institute of Technology,  
Atlanta, GA 30332, USA

<sup>3</sup> Department of Civil and Environmental Engineering, Virginia Polytechnic Institute  
and State University, Blacksburg, VA 24061, USA

\* yang.wang@ce.gatech.edu

## ABSTRACT

This research studies the wireless strain sensing performance of a slotted patch antenna sensor. In our previous work, a folded patch antenna was designed for passive wireless strain and crack sensing. When experiencing deformation, the antenna shape changes, causing shift in electromagnetic resonance frequency of the antenna. The wireless interrogation system utilizes the principle of electromagnetic backscattering and adopts off-the-shelf 900MHz radiofrequency identification (RFID) technology. In this research, a new slotted patch antenna sensor is designed and tested. The antenna detours surface current using slot patterns, so that the effective electrical length is kept similar as previous folded patch antenna. As a result, the sensor footprint is reduced and the antenna resonance frequency is maintained within 900MHz RFID band. To accurately describe both mechanical and electromagnetic behaviors of the antenna sensor, a multi-physics coupled simulation approach is pursued. Implemented through a commercial software package, COMSOL, a multi-physics finite element model of the antenna uses the same geometry and meshing for both mechanical and electromagnetic simulations. Wireless strain sensing performance of the antenna is first simulated using the multi-physics model. In addition, experimental tensile tests are performed to investigate the correlation between wirelessly interrogated resonance frequency and the strain experienced by the antenna. The strain sensing performance is tested.

## INTRODUCTION

To assist in condition evaluation of the nation's aging infrastructure, a large amount of research work in structural health monitoring (SHM) has been conducted in recent decades. An SHM system deploys various sensors to measure the operating conditions and responses of a structure. Among all measurable quantities, strain is one of the key performance indicators for the safety condition of many structural components. Current strain sensing technologies include metal foil strain gages, fiber-optic strain sensors, vibrating-wire strain gages, *etc* (Boller *et al.* 2009). Although

these technologies provide relatively accurate measurement in typical applications, the majority of current sensing systems entail lengthy cables. The expensive installation of cabled monitoring systems presents a major hindrance for large-scale/large-area deployment in the field.

In order to achieve cost-effective SHM, researchers have investigated electromagnetic antennas for wireless strain sensing. The basic concept is to correlate electromagnetic resonance frequency change of an antenna with structural deformation. In particular, an antenna has a specific electromagnetic resonance frequency, which is related with the antenna's physical dimension. When the antenna deforms together with a base structure, the antenna resonance frequency changes accordingly. Such change can be interrogated by a wireless reader and used to derive strain. Different types of antennas have been explored for strain sensing, such as circular patch antenna (Daliri *et al.* 2012) and slotted patch antenna (Salmani *et al.* 2011). Although these antenna sensors demonstrate promising strain measurement results, the application is very limited due to lack of proper signal modulation scheme to enable wireless measurement at a relatively large interrogation distance.

To distinguish backscattered sensor signal from unwanted background reflection, radiofrequency identification (RFID) modulation is a commonly used scheme (Finkenzeller 2003). A meander-line antenna integrated with RFID modulation has been designed for wireless strain sensing on non-metallic structures (Occhiuzzi *et al.* 2011), although the demonstrated measurable strain resolutions are not sufficient for most SHM applications. Recently, the authors developed an RFID-based folded patch antenna as a passive wireless strain sensor (Yi *et al.* 2011). The sensing system utilizes the principle of electromagnetic backscattering and adopts a low-cost off-the-shelf RFID chip to reduce the design and manufacturing cost. In addition, a slotted patch RFID antenna sensor is later proposed to reduce the sensor footprint (Yi *et al.* 2013a). The antenna modeling has been performed using a commercial software package, COMSOL, which supports mechanics-electromagnetics coupled simulation (Yi *et al.* 2013b).

In this research, the initial slotted patch antenna design in Yi *et al.* (2013a) is further tuned to improve the antenna gain and thus increase the interrogation distance for passive wireless strain sensing. The slotted patch antenna is modeled using a commercial software package (COMSOL) for mechanics-electromagnetics coupled simulation. Upon fabrication, the sensor is first tested for interrogation distance limit between the sensor and a wireless reader. In addition, the wireless strain sensing performance is validated by tensile tests. The sensor is tested at an interrogation distance of 36 in. The rest of the paper is organized as follows. First, the strain sensing mechanism and design of the slotted patch antenna sensor are reviewed. The multi-physics simulation in COMSOL is then described. After presenting the test results for interrogation distance limit, the paper describes the wireless strain sensing tests. Finally, a summary and discussion of this work are provided.

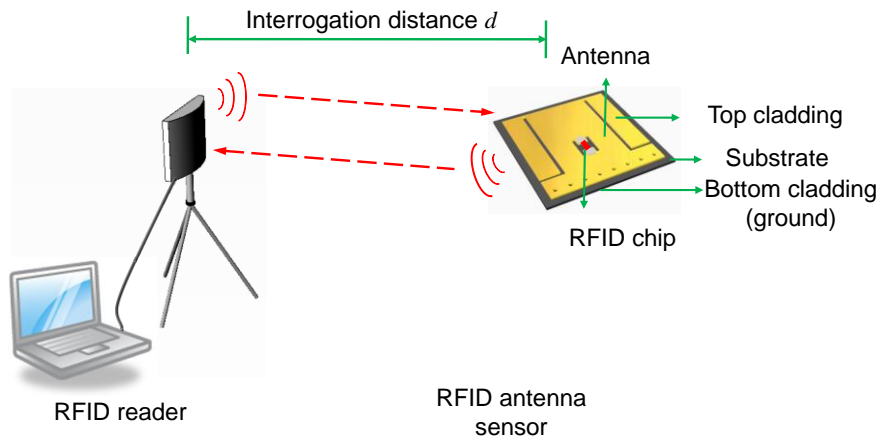
## WIRELESS STRAIN SENSING MECHANISM AND SENSOR DESIGN

As shown in Fig. 1, an RFID sensing system includes a reader and an antenna sensor. The sensor consists of an electromagnetic antenna and an RFID chip for signal modulation. The system operation relies on electromagnetic backscattering. A Tagformance Lite unit (Voyantic 2009) from Voyantic Ltd. is adopted as the RFID reader in this research. During each communication, the reader first emits an interrogation electromagnetic signal. If the antenna sensor is within the interrogation range of the reader, the RFID chip on the antenna sensor captures part of the interrogation power. When the power received at the chip is sufficient, the chip automatically activates and sends modulated electromagnetic signal back to the reader. For every strain measurement, the reader scans through a frequency range and measures the interrogation power threshold that is just sufficient to activate the sensor. The interrogation power threshold is plotted against frequency, and the curve reaches minimum point at the antenna resonance frequency.

Fig. 1 also shows that the antenna consists of three layers, a top metallic cladding (0.7 mil), a dielectric substrate made of Rogers RT/duroid<sup>®</sup> 5880 (31 mils), and a bottom metallic cladding as electrical ground (0.7 mil). The dielectric substrate separates top and bottom metallic layers to form electric field. When the antenna is strain/stress free, the electromagnetic resonance frequency of a half-wavelength patch antenna can be estimated as:

$$f_{R0} = \frac{c}{2L_{\text{eff}} \sqrt{\beta_{\text{reff}}}} \quad (1)$$

where  $c$  is the speed of light,  $L_{\text{eff}}$  is the effective electrical length of the patch antenna, and  $\beta_{\text{reff}}$  is the effective dielectric constant of the substrate. To utilize 900 MHz RFID band (EPCglobal Inc. 2008), the required effective length  $L_{\text{eff}}$  for a patch antenna can be estimated as 4.4 in. (by setting  $f_{R0}$  as 900 MHz, and  $\beta_{\text{reff}}$  as 2.2 for the



Rogers RT/duroid<sup>®</sup> 5880 substrate material). By introducing slots and vias into top cladding, top surface current is detoured. The detouring helps to reduce sensor footprint while achieving a resonance frequency in the 900 MHz band. Using the adopted slot patterns, the effective electrical length of the slotted patch antenna sensor is approximately

$$L_{\text{eff}} = 4(L + L') \quad (2)$$

where  $L$  is the length of the top copper cladding and  $L'$  is the additional electrical length compensating fringing effect.

When the antenna sensor is bonded on a structural surface, the sensor deforms together with the base structure due to applied strain/crack. Because the antenna dimension changes with strain, the antenna resonance frequency shifts with strain. Assuming strain  $\varepsilon$  occurs in the antenna length direction, the resonance frequency shifts to:

$$f_{R\varepsilon} = \frac{c}{8(1 + \varepsilon)(L + L')\sqrt{\beta_{\text{reff}}}} = \frac{f_{R0}}{1 + \varepsilon} \approx f_{R0}(1 - \varepsilon) \quad (3)$$

The equation shows that when strain  $\varepsilon$  is small, the resonance frequency shifting has an approximately linear relationship with strain. This linear relationship indicates that strain can be derived by measuring shift in the antenna resonance frequency. This serves as the fundamental strain sensing mechanism of the RFID antenna sensor.

Due to sensor fabrication and installation tolerance, different pieces of installed sensors usually demonstrate different initial resonance frequencies. To accommodate this variation, the concept of normalized resonance frequency change is defined:

$$\Delta f_N = \frac{f_{R\varepsilon} - f_{R0}}{f_{R0}} \approx -S_N \varepsilon \quad (4)$$

where  $f_{R\varepsilon}$  is the resonance frequency at strain  $\varepsilon$ ,  $\Delta f_N$  is the normalized resonance frequency change, and  $S_N$  is the normalized strain sensitivity. Although according to equations the value of  $S_N$  should be approximately equal to 1, in practice the value is less than 1. This is mainly due to strain transfer effect from the structural surface (being monitored) to the top metallic cladding of the sensor (Yi *et al.* 2011). Only part of the strain experienced by the structure can transfer to the top cladding, whose deformation affects effective electrical length  $L_{\text{eff}}$ .

## MULTI-PHYSICS SIMULATION

To check the antenna sensor performance, the sensor is modeled in COMSOL Multiphysics<sup>™</sup> software package that supports the coupling between mechanics and electromagnetics. Fig. 2 shows the COMSOL simulation model. The slotted patch

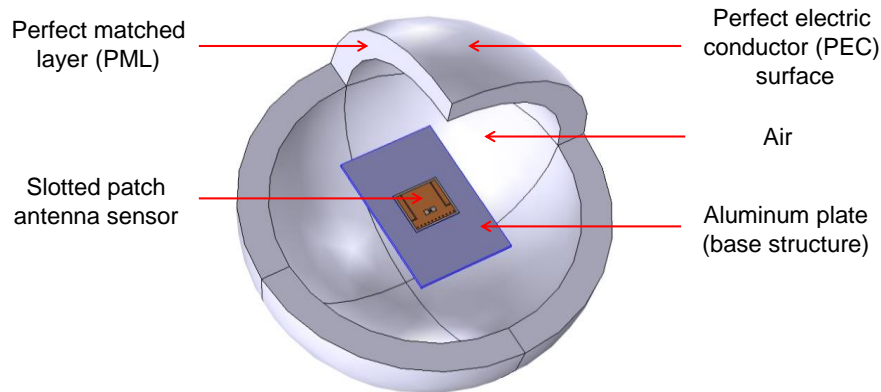


Fig. 2. Simulation model in COMSOL

antenna sensor together with an aluminum plate (base structure) is placed in the center of an air sphere. The boundary conditions can be summarized in two categories, mechanics and electromagnetics. On the mechanics side, the bonding between the antenna sensor and the aluminum plate, as well as the bonding between the copper claddings and the substrate material, is assumed to be ideal (no relative displacement occurs at the interface). To apply strain to the antenna sensor, both ends of the aluminum plate are subject to prescribed uniform displacement in the longitudinal direction, which is the same as the antenna length direction. On the electromagnetics side, boundary condition is set as a perfectly matched layer (PML) at the outer surface of the air sphere. The PML boundary condition allows electromagnetic wave emitted by the antenna sensor to pass through with minimal reflections, which mimics the dissipation of electromagnetic wave into infinite free space. Outside the PML is a perfect electric conductor (PEC) surface to confine the electromagnetics domain to be finite. The RFID chip is simulated as a lumped port with the chip's electrical impedance ( $Z_c = 13.3 - j122 \Omega$ ). Other detailed mechanical and electromagnetic properties of the materials can be found in Yi *et al.* (2013b).

In mechanical simulation, the prescribed displacements at plate ends are adjusted so that seven strain levels (from 0 to  $300\mu\epsilon$ , at an increment step of  $50\mu\epsilon$ ) are sequentially generated in the aluminum plate. After the mechanical simulation at each strain level, COMSOL allows the same deformed meshing to be conveniently reused for electromagnetic simulation. Fig. 3(a) presents the simulated strain distribution in  $y$ -direction on the top copper cladding of the slotted patch antenna sensor, when strain in the aluminum plate is  $100\mu\epsilon$ . Although approximately uniform strain level is achieved around the center area, the strain distribution is not uniform and highly depends on slot patterns. Using the deformed antenna structure, electromagnetic simulation is conducted. Fig. 3(b) illustrates the surface current distribution in  $y$ -direction on the top copper cladding. The figure clearly shows the surface current detouring around the slots and the vias, which confirms the achievement of a longer electrical path while using a smaller sensor footprint.

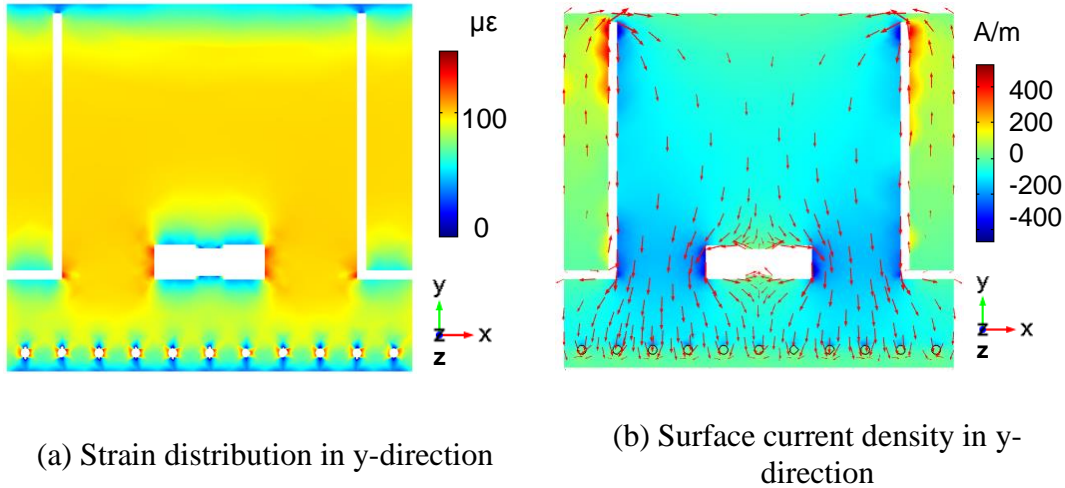


Fig. 3. Field distributions from mechanics-electromagnetics coupled simulation

In the electromagnetic simulation, a frequency domain solver is used to calculate scattering parameter  $S_{11}$ . When the RFID chip emits electromagnetic wave into air through the antenna,  $S_{11}$  equals the ratio between the power reflected by the antenna and the power infused by the RFID chip. Thus, a smaller value of  $S_{11}$  indicates higher antenna efficiency. Fig. 4(a) shows the simulated  $S_{11}$  at all seven strain levels. As expected, the  $S_{11}$  curve and the resonance frequency shift towards left as strain increases. From each  $S_{11}$  curve, the resonance frequency at every strain level is extracted. The normalized frequency is calculated and plotted against strain in Fig. 4(b). Linear regression is performed to the data points. The normalized strain

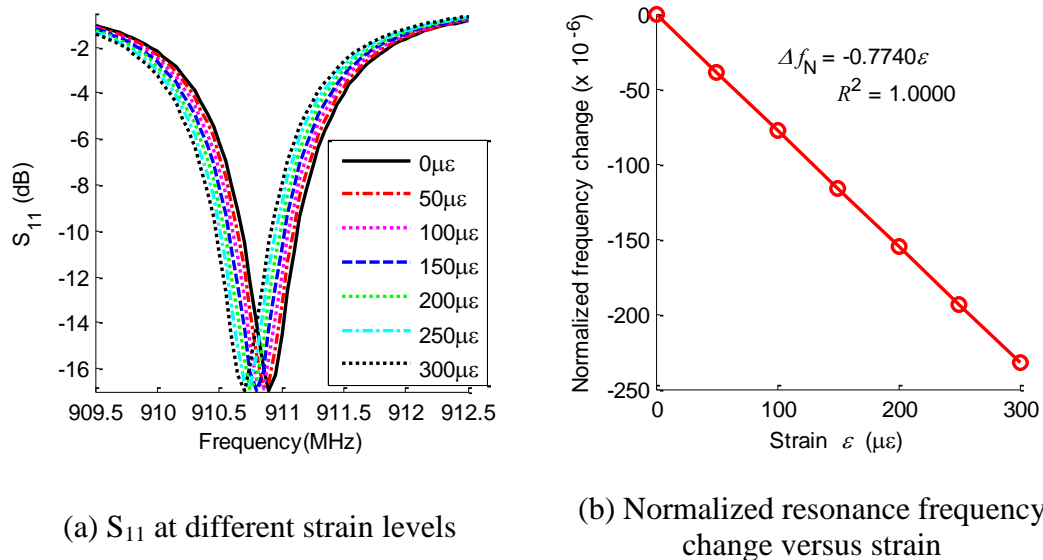


Fig. 4. Simulated resonance frequency change due to strain

sensitivity is  $-0.774$  ppm (part per million)/ $\mu\epsilon$ , which means  $1 \mu\epsilon$  in the aluminum plate causes the resonance frequency to decrease by  $0.774$  ppm. The coefficient of determination ( $R^2$ ) is also calculated to demonstrate the high linearity.

Fig. 5 shows the design drawing and photo of a fabricated slotted patch antenna sensor. The overall size is  $44\text{mm} \times 48\text{mm} \times 0.79\text{mm}$ . Plane dimension of the sensor is about half of the previously developed folded patch antenna sensor (Yi *et al.* 2011).

### INTERROGATION DISTANCE TEST

Interrogation distance test is first conducted to investigate the maximum distance at which the sensor can be wirelessly interrogated by a reader. The slotted patch antenna sensor is bonded to an aluminum plate of  $152\text{mm} \times 700\text{mm} \times 3.18\text{mm}$ . The Tagformance reader together with a high gain Yagi antenna is adopted for interrogation. During the test, the distance between the sensor and the reader antenna is gradually increased from 12in. to 90 in., in seven steps. At each distance, the

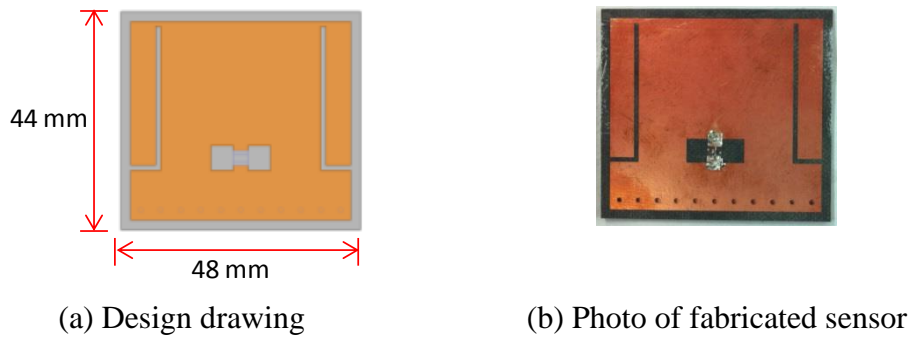


Fig. 5. Slotted patch antenna sensor

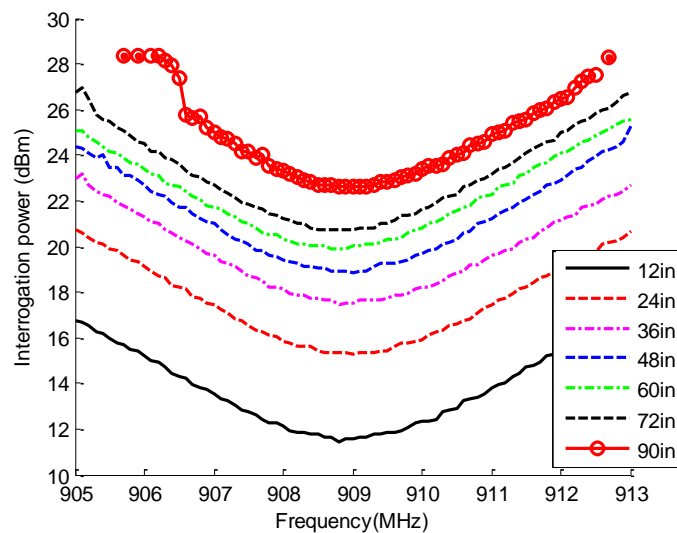


Fig. 6. Interrogation power threshold at different interrogation distances

interrogation power threshold of the sensor is obtained by the reader. Fig. 6 presents the interrogation power threshold plot at different interrogation distances. When the interrogation distance is 12 in., the interrogation power threshold around the resonance frequency is less than 12 dBm, meaning a lower interrogation power is needed to activate the passive sensor. When the interrogation distance increases up to 90 in., the reader is still capable of measuring 3dB bandwidth (needed for reliably extracting resonance frequency) of the interrogation power curve. Meanwhile, the power level around the resonance frequency increases to about 23 dBm, i.e. larger interrogation power is needed at a longer distance.

## WIRELESS STRAIN SENSING PERFORMANCE

After the interrogation distance test, strain sensing performance of the antenna is validated by tensile tests. Fig. 7(a) shows configuration of the experimental specimen, where a slotted patch antenna sensor together with five metal foil strain gages are installed at the center of an aluminum plate. Fig. 7(b) shows the experimental setup for wireless strain sensing. A Yagi reader antenna, connected with the Tagformance reader, faces the center of the antenna sensor at a distance of 36 in. The tensile loading is configured so that about 50  $\mu\epsilon$  increment is generated between two adjacent loading steps. At each loading step, the interrogation power threshold is obtained by the reader. Meanwhile, the strain data from the metal foil strain gages are measured by the NI (National Instruments) data acquisition system as baseline reference.

Although seven strain levels are tested, for clarity, interrogation power threshold for only four strain levels is plotted in Fig. 8(a). The resonance frequency gradually shifts towards left as strain increases. A fourth-order curve fitting is applied to the peak area of these curves and the resonance frequency is extracted from the

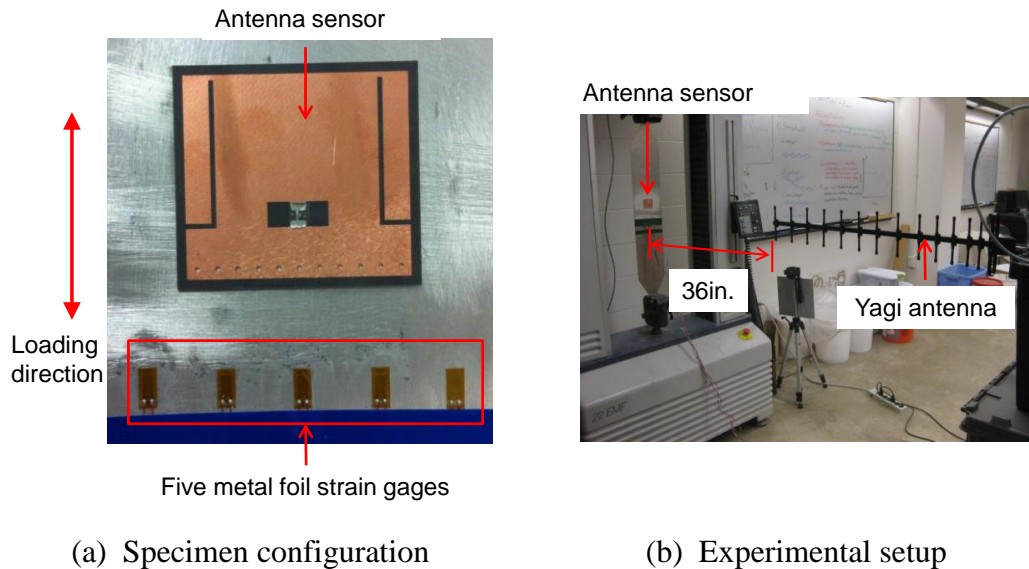


Fig. 7. Experimental setup for the tensile test of a slotted patch antenna



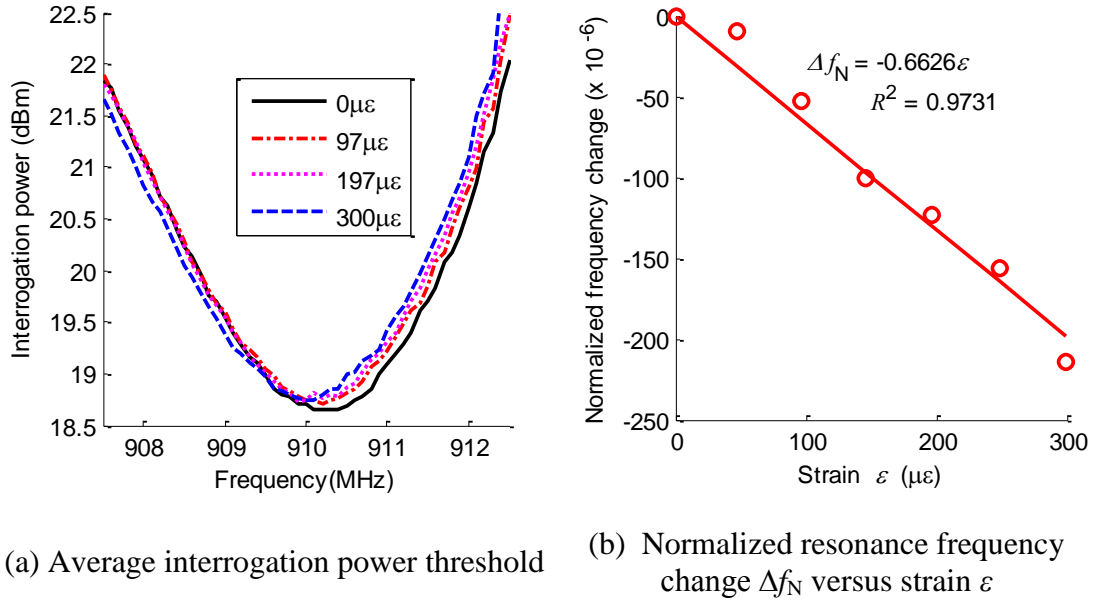


Fig. 8. Tensile testing results at 36 in. interrogation distance

fitted curves (Yi *et al.* 2011). The resonance frequency changes are then normalized according to Eq. (4), and plotted for each strain level in Fig. 8(b). The figure shows the normalized strain sensitivity is  $-0.6626$  ppm/ $\mu\varepsilon$ . The result is close to the sensitivity of the previous folded patch antenna sensor (Yi *et al.* 2011). The corresponding coefficient of determination is 0.9731, which indicates acceptable linearity. Comparison between Fig. 8(b) and Fig. 4(b) shows the experimental sensitivity is slightly lower than the simulated sensitivity. The difference may be due to the imperfect bonding between the antenna sensor and the aluminum specimen. Furthermore, because microscopic voids always exist in the substrate material, when under strain, the effective dielectric constant  $\beta_{\text{reff}}$  may vary due to the distortion of the voids. This variation of  $\beta_{\text{reff}}$  also affects the resonance frequency, and the effect needs to be studied in the future.

## SUMMARY AND CONCLUSIONS

In this research, a slotted patch antenna sensor is designed and tested. Mechanics-electromagnetics coupled simulation is conducted to accurately model the strain sensing performance. Compared with the previous folded patch antenna sensor, the sensor footprint is reduced by introducing slot patterns on the top copper cladding. Upon fabrication, interrogation distance test shows the sensor can operate up to 90 in. away from a wireless reader. In addition, tensile tests demonstrate that the sensor provides acceptable strain sensing performance in terms of sensitivity and linearity. In the future, more exhaustive tests could be conducted to fully investigate the sensor performance in wireless strain sensing resolution, strain measurement range, crack

propagation tracking, etc. Furthermore, to improve the interrogation distance, an active RFID chip together with a solar cell can be investigated for incorporation with the antenna sensor.

## ACKNOWLEDGEMENT

This material is based upon work supported by the Federal Highway Administration under agreement No. DTFH61-10-H-00004. Any opinions, findings, and conclusions or recommendations expressed in this publication are those of the authors and do not necessarily reflect the view of the sponsor.

## REFERENCES

- Boller, C., Chang, F.-K., and Fujino, Y. (2009). *Encyclopedia of Structural Health Monitoring*. Wiley & Sons, Inc.
- Daliri, A., Galehdar, A., John, S., Wang, C. H., Towe, W. S. T., and Ghorbani, K. (2012). "Wireless strain measurement using circular microstrip patch antennas." *Sensors and Actuators A: Physical*, 184, 86-92.
- EPCglobal Inc. (2008). *EPC™ Radio-frequency Identity Protocols Class-1 Generation-2 UHF RFID Protocol for Communications at 860 MHz-960 MHz* Version 1.2.0, EPCglobal Inc.
- Finkenzeller, K. (2003). *RFID Handbook*. John Wiley & Sons, New York.
- Occhiuzzi, C., Paggi, C., and Marrocco, G. (2011). "Passive RFID strain-sensor based on meander-line antennas." *IEEE Transactions on Antennas and Propagation*, 59(12), 4836-4840.
- Salmani, Z., Xie, Y., Zheng, G., Zhang, H., and Zhang, H. (2011). "Application of Antenna in Strain Measurement." *Proceedings of 2011 International Workshop on Antenna Technology (IWAT)*, Hong Kong, 336-339.
- Voyantic. (2009). *Tagformance Lite Measurement System User Guide*. Voyantic Ltd., Espoo, Finland.
- Yi, X., Wu, T., Wang, Y., Leon, R. T., Tentzeris, M. M., and Lantz, G. (2011). "Passive wireless smart-skin sensor using RFID-based folded patch antennas." *International Journal of Smart and Nano Materials*, 2(1), 22-38.
- Yi, X., Cho, C., Cook, B., Wang, Y., Tentzeris, M. M., and Leon, R. T. (2013a). "Design and simulation of a slotted patch antenna sensor for wireless strain sensing." *Proceedings of SPIE, Nondestructive Characterization for Composite Materials, Aerospace Engineering, Civil Infrastructure, and Homeland Security*, San Diego, California, USA, 86941J.
- Yi, X., Wang, Y., Tentzeris, M. M., and Leon, R. T. (2013b). "Multi-physics modeling and simulation of a slotted patch antenna for wireless strain sensing." *Proceedings of the 9th International Workshop on Structural Health Monitoring (IWSHM)*, Stanford, CA, USA, 1857-1864.